Mathematical Biosciences and Engineering

http://www.aimspress.com/journal/mbe

MBE, 20(4): 7171–7192.
DOI: 10.3934/mbe.2023310
Received: 08 December 2022
Revised: 20 January 2023
Accepted: 02 February 2023
Published: 10 February 2023

Research article

Patch model for border reopening and control to prevent new outbreaks of COVID-19

Tingting Zheng[1,*], Huaiping Zhu[3,*], Zhidong Teng[1], Linfei Nie[2], and Yantao Luo[2]

[1] College of Medical Engineering and Technology, Xinjiang Medical University, Urumqi, PR China
[2] College of Mathematics and Systems Science, Xinjiang University, Urumqi, PR China
[3] Department of Mathematics and Statistics, York University, Toronto, Canada

* **Correspondence:** Emails:ztt0711@163.com; huaiping@yorku.ca.

Abstract: In this paper, we propose a two-patch model with border control to investigate the effect of border control measures and local non-pharmacological interventions (NPIs) on the transmission of COVID-19. The basic reproduction number of the model is calculated, and the existence and stability of the boundary equilibria and the existence of the coexistence equilibrium of the model are obtained. Through numerical simulation, when there are no unquarantined virus carriers in the patch-2, it can be concluded that the reopening of the border with strict border control measures to allow people in patch-1 to move into patch-2 will not lead to disease outbreaks. Also, when there are unquarantined virus carriers in patch-2 (or lax border control causes people carrying the virus to flow into patch-2), the border control is more strict, and the slower the growth of number of new infectious in patch-2, but the strength of border control does not affect the final state of the disease, which is still dependent on local NPIs. Finally, when the border reopens during an outbreak of disease in patch-2, then a second outbreak will happen.

Keywords: COVID-19; Patch model; Border control; reopen border

1. Introduction

It is reported that from the COVID-19 epidemic in the past three years, and due to the huge number of infected people, hundreds of variants have been produced, among which the most adaptable variant has become the global epidemic strain. From the early original strain to the Omicron strain, these variations are all generated through continuous evolution. This pathogen represents a substantial challenge for public health, pandemic planning and health care systems. According to real-time data from Worldometer, as of October 17, 2022, there were 629,958,941 confirmed COVID-19 cases and 6,571,478 deaths worldwide [1].

It is known to all that people all over the world have been widely vaccinated with the novel coronavirus vaccine to establish their own immune barrier; however, vaccination seems to only reduce the infection rate and reduce the severity, but not provide complete immunity to the virus [2]. In the absence of specific drugs against COVID-19, mitigating the epidemic will depend on non-pharmacological interventions(NPIs). There are many kinds of NPIs, which can be divided into two levels: one is the personal level, such as home quarantine, social distancing, wearing masks, and frequent hand washing; and the other level of the disease control department, such as tracking close contacts, controlling foreign personnel (returning home, traveling or visiting) and so on.

Mathematical models for the COVID-19 pandemic have been proposed to assess the effectiveness of NPIs and study the dynamic behavior of the pandemic. For example, Seungpil et al. [3] proposed a modified SEIR model to assess the effectiveness of social distancing, ban on gatherings and vaccination strategies. Studies by Chinazzi et al. [4] have shown that additional travel restrictions (up to 90% of traffic) have only a modest effect, unless coupled with public health interventions and behavioral changes, can significantly reduce the rate of disease transmission. For other related research results, see Refs.([3–7]) and the references therein.

As we know, many countries and regions in the world have implemented lockdowns to curb the rapid spread of COVID-19, and achieved phased victory at the early stage of the outbreak. For example, Yang et al. [8] established a mathematical model and estimated that the opportunity of COVID-19 transmission will be reduced after the implementation of mandatory control measures on January 23, 2020; however, if the mandatory measures, such as "closed city", are postponed for 5 days, the epidemic scale on the Chinese mainland will expand three times. However, with the universal vaccination of the new coronavirus vaccine, people's immune system has been gradually established. In addition, the mortality rate of the mutant virus Omicron has decreased, and many places are planning to lift the closure (schools, work places, businesses), including reopening of borders between countries, provinces, and regions. In fact, the reopening or lifting are still risky due to the fast spreading, and in particularly, the higher percentage of asymptomatic infected individuals. It is essential to assess the risk of lifting, and quantify the threshold conditions to inform the decision-making of public health. Further, there are differences in the ability of responding to public health emergencies, medical resources, relevant policies and the degree of residents' compliance with policies in every country and even every city.

Hence, there are some patch models that are proposed to depict the spread of disease from one region to another, or in multiple-regions, see Refs.([9–12]). For instance, Sun et al. [10] proposed a two-patches model to reflect the mobility of humans between Hubei and regions outside Hubei, and estimated the effective reproduction numbers for two patches, and also discussed the impact of the resumption of work and production in Wuhan and the lifting of lockdown on the spread of COVID-19. In particular, Hu et al [11] proposed a two-patches mathematical model to investigate the effects of migration and supply of medical resources on the transmission of disease. However, as far as we know, most of the above mentioned patch model studies on COVID-19 focus on the dynamic impact of human activities on disease transmission between patches, and few study the impact of the severity of various control measures between patches on disease transmission.

Hence, in this paper, we will take the movement of non-quarantined individuals from one patch to the other and border controls into consideration, and propose a two-patch model to study the impact of the severity of various control measures between patches on disease transmission. The details can

be found in the following sections. In Section 2, we first propose a single patch model without population movement and study its basic properties, and then extend this model to a two-patch model by considering border reopening and border control. We investigate the threshold dynamics of the border reopening model in Section 3. Finally, we give some numerical simulation and a brief discussion in Section 4 and Section 5, respectively.

2. Modelling

In this paper, we consider two closely related regions (cities, countries). During the COVID-19 outbreak, many countries have resorted to city closures, or even country closures, to avoid wider spread of the epidemic and to accelerate local control. Therefore, this section will be divided into two subsections to discuss changes in control measures for controlling the spread of disease when borders are closed and reopened.

2.1. Without population movement

Regardless of the population movement between the two patches, that is, the two patches are independent of each other, and each has its own NPIs measures, we consider the situation that the epidemic of COVID-19 in both patches are under control, otherwise, there is no reason to open the border to allow population movement.

The latent period is shorter than incubation period for COVID-19. A person can transmit infection without showing any signs of the disease. Such infection is called subclinical infection [14]. Therefore, we divide the human population on each patch-j ($j = 1, 2$) into the following classes: susceptible ($S_j(t)$), exposed ($E_j(t)$), subclinical infection ($I_{aj}(t)$) (include those who remain asymptomatic and those who have not yet developed symptoms), symptomatic infectious ($I_j(t)$), quarantined and hospitalized ($H_j(t)$) who are all severely infected, and recovered ($R_j(t)$).

Considering the following two types of forced quarantine: quarantine of traced close contacts (including susceptible, exposed, and subclinical infected), and quarantine of confirmed infected individuals with mild clinical symptoms. Let $S_{qj}(t)$ denote quarantined susceptible (close contacts identified), after the period of forced quarantine, people will return to class $S_j(t)$. Let $Q_j(t)$ denote quarantined carriers of the virus, in which they either develop mild symptoms and then recover, or develop severe symptoms and are hospitalized. In this paper, we assume that infected with severe cases will be admitted to designated hospitals for treatment, while confirmed infected individuals with mild symptoms and traced carriers of the virus will be sent to the centralized observation places for centralized quarantine.

For the patch-j ($j = 1, 2$) population, people enter the susceptible class through birth at a recruitment rate Λ_j, and leave all classes through the same natural death rate μ. When a susceptible individual comes into contact with an infectious individual, there is some probability that the person can get the virus and move to the exposed class at the infection rate $c_j\beta_j\left(I_{aj} + I_j\right)$. Here, c_j is the contact rate in patch-j, and β_j is the probability of transmission per contact in patch-j. Let τ and σ be the transition rate of exposed individuals to the subclinical infection and the transition rate of subclinical infection to the infected with symptom class, respectively. The terms θ_j and δ_j represent the rate of hospitalizations due to severe clinical symptoms in the class of I_j and in the class of Q_j, respectively. When the infected individuals with severe clinical symptoms are admitted to the hospital, they move to the recovered class at a rate γ_{hj}, and die from infection at a rate d_j. Furthermore, γ_a, γ and γ_{qj} are recovered

rates in subclinical infected, symptomatic infected and quarantined carriers of the virus, respectively.

Moreover, q_{sj}, q_{ej}, q_{aj} and q_{ij} are the forced quarantine rate of susceptible individuals, exposed individuals, subclinical infected and symptomatic infected by contact tracing, respectively. η_j denotes the rate of the quarantined uninfected contacts of patch-j . The flowchart of COVID-19 transmission for patch-j ($j = 1, 2$) without population movement is illustrated in Figure 1. Based on the above assumptions and the flow chart, we propose the following single patch model (2.1)-(2.2) for patch-j ($j = 1, 2$):

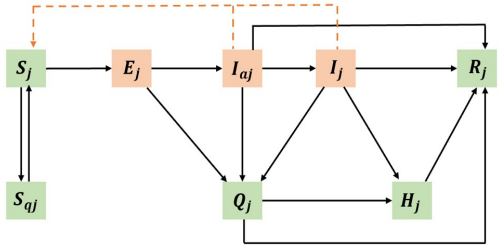

Figure 1. Flow diagram of the COVID-19 model in patch-j. Solid lines indicate the movement between classes. Dashed lines represent the virus transmission routes.

$$\begin{cases} \dfrac{\mathrm{d}S_j}{\mathrm{d}t} = \Lambda_j - c_j\beta_j S_j\left(I_{aj} + I_j\right) - \left(q_{sj} + \mu\right) S_j + \eta_j S_{qj}, \\ \dfrac{\mathrm{d}E_j}{\mathrm{d}t} = c_j\beta_j S_j\left(I_{aj} + I_j\right) - \left(\tau + q_{ej} + \mu\right) E_j, \\ \dfrac{\mathrm{d}I_{aj}}{\mathrm{d}t} = \tau E_j - \left(\gamma_a + \sigma + q_{aj} + \mu\right) I_{aj}, \\ \dfrac{\mathrm{d}I_j}{\mathrm{d}t} = \sigma I_{aj} - \left(\theta_j + \gamma + q_{ij} + \mu\right) I_j, \\ \dfrac{\mathrm{d}S_{qj}}{\mathrm{d}t} = q_{sj} S_j - \left(\eta_j + \mu\right) S_{qj}, \end{cases} \tag{2.1}$$

and

$$\begin{cases} \dfrac{\mathrm{d}Q_j}{\mathrm{d}t} = q_{ej}E_j + q_{aj}I_{aj} + q_{ij}I_j - \left(\delta_j + \gamma_{qj} + \mu\right) Q_j, \\ \dfrac{\mathrm{d}H_j}{\mathrm{d}t} = \theta_j I_j + \delta_j Q_j - \left(\gamma_{hj} + d_j + \mu\right) H_j, \\ \dfrac{\mathrm{d}R_j}{\mathrm{d}t} = \gamma_{aj} I_{aj} + \gamma I_j + \gamma_{qj} Q_j + \gamma_{hj} H_j - \mu R_j. \end{cases} \tag{2.2}$$

It is obvious that Q_j, H_j and R_j can be decoupled from the other equations in model (1), so it suffices to only study model (2.1). Associated with model (2.1), we also consider the following initial conditions:

$$S_j(0) > 0,\ E_j(0) \geq 0,\ I_{aj}(0) \geq 0,\ I_j(0) \geq 0,\ S_{qj}(0) \geq 0.$$

It is easy to calculate that model (2.1) always has a disease-free equilibrium $e_{0j} = (s_j^*, 0, 0, 0, s_{qj}^*)$, where $s_j^* = \frac{\Lambda_j(\eta_j+\mu)}{\mu(\eta_j+q_{sj}+\mu)}$, $s_{qj}^* = \frac{\Lambda_j q_{sj}}{\mu(\eta_j+q_{sj}+\mu)}$. Then, using the next generation method, we obtain the basic reproduction number of model (2.1):

$$\mathcal{R}_{0j} = \frac{c_j\beta_j s_j^* \tau\left(\theta_j + \gamma + q_{ij} + \mu + \sigma\right)}{\left(\theta_j + \gamma + q_{ij} + \mu\right)\left(\gamma_a + \sigma + q_{aj} + \mu\right)\left(\tau + q_{ej} + \mu\right)}.$$

The properties of equilibria of model (2.1) are given in the following theorem:

Theorem 2.1. (*i*) *If* $\mathcal{R}_{0j} < 1$*, then disease-free equilibrium* e_{0j} *is globally asymptotically stable.*

(*ii*) *If* $\mathcal{R}_{0j} > 1$*, then disease-free equilibrium* e_{0j} *is unstable, and model* (2.1) *has a unique endemic equilibrium* $e_j^* = (s_j^{**}, e_j^{**}, i_{aj}^{**}, i_j^{**}, s_{qj}^{**})$*, where*

$$
\begin{aligned}
s_j^{**} &= \frac{\left(\mu+\tau+q_{ej}\right)\left(\mu+\theta_j+\gamma+q_{ij}\right)\left(\mu+\gamma_a+\sigma+q_{aj}\right)}{c_j\beta_j\tau\left(\mu+\theta_j+\gamma+q_{ij}+\sigma\right)},\\
e_j^{**} &= \frac{\mu\left(\eta+\mu+q_{sj}\right)\left(\mu+\theta_j+\gamma+q_{ij}\right)\left(\mu+\gamma_a+\sigma+q_{aj}\right)\left(\mathcal{R}_{0j}-1\right)}{c_j\beta_j\tau\left(\mu+\eta_j\right)\left(\mu+\theta_j+\gamma+q_{ij}+\sigma\right)},\\
i_{aj}^{**} &= \frac{\mu\left(\eta+\mu+q_{sj}\right)\left(\mu+\theta_j+\gamma+q_{ij}\right)\left(\mathcal{R}_{0j}-1\right)}{c_j\beta_j\left(\mu+\eta_j\right)\left(\mu+\theta_j+\gamma+q_{ij}+\sigma\right)},\\
i_j^{**} &= \frac{\mu\sigma\left(\eta+\mu+q_{sj}\right)\left(\mathcal{R}_{0j}-1\right)}{c_j\beta_j\left(\mu+\eta_j\right)\left(\mu+\theta_j+\gamma+q_{ij}+\sigma\right)},\\
s_{qj}^{**} &= \frac{q_{sj}\left(\mu+\tau+q_{ej}\right)\left(\mu+\theta_j+\gamma+q_{ij}\right)\left(\mu+\gamma_a+\sigma+q_{aj}\right)}{c_j\beta_j\tau\left(\mu+\eta_j\right)\left(\mu+\theta_j+\gamma+q_{ij}+\sigma\right)}.
\end{aligned}
$$

That is to say, if $\mathcal{R}_{0j} < 1$, then the disease will go extinct in patch-j, and the disease become endemic in patch-j when $\mathcal{R}_{0j} > 1$. When the border is closed, we can adopt the local NPIs policies to control the basic reproduction number, so as to control the spread of COVID-19 in patch-j. Then, naturally, we will consider how the reopening of the border will affect the epidemic in patch-j if the epidemic situation in patch-j is controlled. Is it still effective to continue to take local NPIs measures after reopening the border?

2.2. Border control for reopening

For the above two patches, when the basic reproduction number of one patch is less than 1, the patch can consider reopening the border to allow people from the other patch to move into the patch with border control measures. That is assuming that $\mathcal{R}_{02} < 1$ meaning the patch-2 allows the people of patch-1 to move in under some border control measures. For the patch-$i(i = 1, 2)$, we classify the general population into the following groups: susceptible (S_i), exposed (E_i), subclinical infection (I_{ai}), symptomatic infection (I_i), centralized quarantine susceptible (S_{qi}), centralized quarantine carriers of the virus (Q_i), hospitalized (H_i) and recovered (R_i). We subdivide the centralized quarantine population at entry into four classes: susceptible (S_w), exposed (E_w), subclinical infection (A_w) and symptomatic infection (I_w).

During the outbreak of COVID-19, we consider only people in high-risk areas moving to low risk area. There are two ways for entry: conventional entry and unconventional entry. People who conventional entry must accept entry centralized quarantine for a while (usually for 14 days), with one room per person (i.e., there are no new infections in the quarantine places at entry). People are tested for nucleic acids at least twice during centralized quarantine. Unconventional entry individuals are not subject to centralized quarantine and go directly to local areas. Let ρ $(0 \le \rho \le 1)$ represent the rate

of conventional entry by individuals in various classes. Here, $\rho = 1$ means that entry control measures in a low-risk area is very strict and there is no unconventional entry individuals, and $\rho = 0$ means that no entry control measures have been taken in a low-risk area. The flow diagram of the patch-model is shown in Figure 2. We propose the following assumptions:

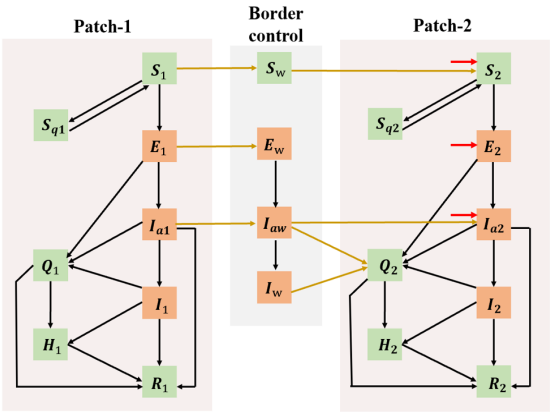

Figure 2. Flow diagram of the COVID-19 model in two-patch with border control. The red arrows in the figure represent the portion of unconventional entry individuals from patch-1 to patch-2.

(A_1) 100% of symptomatic infectious individuals can be detected during entry quarantine, and a small number of subclinical infectious individuals may not be detected.

(A_2) The entry quarantine period is not too long, ignoring the natural birth rate and natural death rate of the population during the period of entry quarantine.

(A_3) People who recover from COVID-19 will not be re-infected. We ignore the migration of people who have recovered because the probability of them moving from one country to another during the epidemic is very small.

(A_4) Once the infected is diagnosed at the entry quarantine places, they will be transferred to the local quarantine observation places for non-severe symptoms, thus entering the Q compartment.

(A_5) The reason why people leave the entry quarantine place is because the susceptible individuals leave after the expiry of the quarantine period, or the infected individuals are transferred to the local centralized quarantine observation places with a positive nucleic acid test.

Base on the above assumption and the flow diagram in Figure 2, we arrive at the following equations

for each subpopulation from patch-i:

$$
\begin{cases}
\begin{cases}
\dfrac{\mathrm{d}S_1}{\mathrm{d}t} = \Lambda_1 - c_1\beta_1 S_1 (I_{a1} + I_1) - (\mu + q_{s1}) S_1 + \eta_1 S_{q1} - mS_1, \\
\dfrac{\mathrm{d}E_1}{\mathrm{d}t} = c_1\beta_1 S_1 (I_{a1} + I_1) - (\tau + \mu + q_{e1}) E_1 - mE_1, \\
\dfrac{\mathrm{d}I_{a1}}{\mathrm{d}t} = \tau E_1 - (\gamma_a + \sigma + \mu + q_{a1}) I_{a1} - mI_{a1}, \\
\dfrac{\mathrm{d}I_1}{\mathrm{d}t} v = \sigma I_{a1} - (\theta_1 + \gamma + \mu + q_{i1}) I_1, \\
\dfrac{\mathrm{d}S_{q1}}{\mathrm{d}t} = q_{s1} S_1 - (\eta_1 + \mu) S_{q1},
\end{cases} \\
\begin{cases}
\dfrac{\mathrm{d}S_w}{\mathrm{d}t} = m\rho S_1 - \kappa S_w, \\
\dfrac{\mathrm{d}E_w}{\mathrm{d}t} = m\rho E_1 - \tau_w E_w, \\
\dfrac{\mathrm{d}I_{aw}}{\mathrm{d}t} = m\rho I_{a1} + \tau_w E_w - (\sigma_w + q_{aw} + \epsilon) I_{aw}, \\
\dfrac{\mathrm{d}I_w}{\mathrm{d}t} = \sigma_w I_{aw} - q_{iw} I_w,
\end{cases} \\
\begin{cases}
\dfrac{\mathrm{d}S_2}{\mathrm{d}t} = \Lambda_2 + m(1-\rho) S_1 + \kappa S_w - c_2\beta_2 S_2 (I_{a2} + I_2) - (\mu + q_{s2}) S_2 + \eta_2 S_2, \\
\dfrac{\mathrm{d}E_2}{\mathrm{d}t} = m(1-\rho) E_1 + c_2\beta_2 S_2 (I_{a2} + I_2) - (\tau + \mu + q_{e2}) E_2, \\
\dfrac{\mathrm{d}I_{a2}}{\mathrm{d}t} = m(1-\rho) I_{a1} + \tau E_2 + \epsilon I_{aw} - (\gamma_a + \sigma + \mu + q_{a2}) I_2, \\
\dfrac{\mathrm{d}I_2}{\mathrm{d}t} = \sigma I_{a2} - (\theta_2 + \gamma + \mu + q_{i2}) I_2, \\
\dfrac{\mathrm{d}S_{q2}}{\mathrm{d}t} = q_{s2} S_2 - (\eta_2 + \mu) S_{q2},
\end{cases}
\end{cases}
\tag{2.3}
$$

and

$$
\begin{cases}
\begin{cases}
\dfrac{\mathrm{d}Q_1}{\mathrm{d}t} = q_{e1} E_1 + q_{a1} I_{a1} + q_{i1} I_1 - \left(\delta_1 + \gamma_{q1} + \mu\right) Q_1, \\
\dfrac{\mathrm{d}H_1}{\mathrm{d}t} = \theta_1 I_1 + \delta_1 Q_1 - (\gamma_{h1} + d_1 + \mu) H_1, \\
\dfrac{\mathrm{d}R_1}{\mathrm{d}t} = \gamma_a I_{a1} + \gamma I_1 + \gamma_{q1} Q_1 + \gamma_{h1} H_1 - \mu R_1,
\end{cases} \\
\begin{cases}
\dfrac{\mathrm{d}Q_2}{\mathrm{d}t} = q_{e2} E_2 + q_{a2} I_{a2} + q_{i2} I_2 + q_{aw} I_{aw} + q_{iw} I_w - \left(\delta_2 + \gamma_{q2} + \mu\right) Q_2, \\
\dfrac{\mathrm{d}H_2}{\mathrm{d}t} = \theta_2 I_2 + \delta_2 Q_2 - (\gamma_{h2} + d_2 + \mu) H_2, \\
\dfrac{\mathrm{d}R_2}{\mathrm{d}t} = \gamma_a I_{a2} + \gamma I_2 + \gamma_{q2} Q_2 + \gamma_{h2} H_2 - \mu R_2.
\end{cases}
\end{cases}
\tag{2.4}
$$

The parameters in this model are described in Table 1. It is obvious that Q_1, H_1, R_1, Q_2, H_2 and R_2 can be decoupled from all the equations in model (2.3), so it is suffices to study model (2.3). The

initial value for all populations in model (2.3) is given by:

$$S_i > 0,\ E_i \geq 0,\ I_{ai} \geq 0,\ I_i \geq 0,\ S_{qi} \geq 0,\ S_w \geq 0,\ E_w \geq 0,\ I_{aw} \geq 0,\ I_{aw} \geq 0,\ i = 1, 2. \tag{2.5}$$

Table 1. Definition and possible values of the basic parameter for model (2.3).

Param.	Description	Value	Source
Λ_1/Λ_2	Recruitment rate of human in patch-1,2	Variable	–
c_1/c_2	Contact rate in patch-1,2	[5,14]	[15]
β_1/β_2	Probability of transmission per contact in patch-1,2		
$q_{sj}, q_{ej}, q_{aj}, q_{ij}$	The force quarantine rate of class S_j, E_j,I_{aj},I_j, j=1,2	$[0, 1)$	–
q_{aw}, q_{iw}	The transfer rate of from I_{aw}, I_w classes to Q_2	$[0, 1)$	–
θ_1/θ_2	Rate of hospitalizations in the class of I_1/I_2	0.0152	[16]
η_1/η_2	Rate of the quarantined uninfected contacts in patch-1,2	$(0, 0.14)$	–
δ_1/δ_2	Rate of hospitalizations in the class of Q_1/Q_2	0.02	-
γ_{q1}/γ_{q2}	Recovery rate of the class of Q_1/Q_2	$(0.0775, 0.1549)$	[16]
γ_{h1}/γ_{h2}	Recovery rate of the class of H_1/H_2	$(0.0357, 0.17)$	[16]
d_1/d_2	Disease-induced death rate of human in patch-1,2	$(0.0051, 0.0056)$	[17]
μ	Natural death rate of human	$1/(78 * 365)$	–
m	Move rate of human from patch-1 to patch-2	$(0, 1)$	-
τ	Transition rate of exposed to subclinical infection	$[0.2, 0.25]$	[18]
γ_a	Recovery rate of subclinical infection	$(0.06929, 0.0708)$	[17]
σ	Transition rate of E_i class to I_i class, $i = 1, 2$	0.33	-
γ	Recovery rate of symptomatic infection	0.07	[17]
ρ	Rate of conventional entry individuals in various classes	$(0, 1)$	-
κ	Transition rate of from S_w to S_2	$1/14$	-
τ_w	Transition rate of exposed individuals to subclinical infection at the border quarantine places	$(0, 0.25)$	-
σ_w	Transition rate of subclinical infection to symptomatic infection at the border quarantine places	$(0, 0.33)$	-
ϵ	Rate of subclinical infections that are not detected at the border quarantine places	$[0, 1 - \sigma_w - q_{aw})$	-

On the positivity and boundedness of solutions for model (2.3), we have the following result, which can be easily proved by using a similar argument as in [19, Theorem 3.1]:

Theorem 2.2. *Let* $X(t) = (S_1(t), E_1(t), I_{a1}(t), I_1(t), S_{q1}(t), S_w(t), E_w(t), I_{aw}(t), I_w(t), S_2(t), E_2(t), I_{a2}(t), I_2(t), S_{q2}(t))$ *be the solution of model* (2.3) *with initial condition* (2.5)*. Then, we have*

(*a*) $X(t)$ *is nonnegative for all* $t \geq 0$ *and ultimately bounded;*

(*b*) *If* $X(0) > 0$, *then* $X(t)$ *is also positive for all* $t > 0$.

Remark 2.1. It is easy to verify that when the initial value of unquarantine carriers of the virus in patch-2 is equal to zero ($E_2(0) = I_{a2}(0) = I_2(0) = 0$), it can be obtained from model (2.3) that the number of newly infected individuals is equal to zero for $t \geq 0$. That is to say, under strict border control measures, border reopening will not result in an outbreak of patch-2 disease (all carriers of the virus are detected at the border quarantine places, sent to the hospital and quarantined, and no new infections will occur locally). This is different from other patch models of infectious diseases [20–23].

3. Threshold dynamics

In this section, we focus on the basic reproduction number of model (2.3), the stability of disease-free equilibrium and boundary equilibrium, and the existence of coexistence equilibrium. Firstly, when

$E_i = 0, I_{ai} = 0$ and $I_i = 0$ $(i = 1, 2, w)$, we have the disease-free subsystem

$$\begin{cases} \dfrac{\mathrm{d}S_1}{\mathrm{d}t} = \Lambda_1 - (\mu + q_{s1})\, S_1 + \eta_1 S_{q1} - mS_1, \\ \dfrac{\mathrm{d}S_{q1}}{\mathrm{d}t} = q_{s1} S_1 - (\eta_1 + \mu)\, S_{q1}, \\ \dfrac{\mathrm{d}S_w}{\mathrm{d}t} = m\rho S_1 - \kappa S_w, \\ \dfrac{\mathrm{d}S_2}{\mathrm{d}t} = \Lambda_2 + m(1-\rho) S_1 + \kappa S_w - (\mu + q_{s2})\, S_2 + \eta_2 S_2, \\ \dfrac{\mathrm{d}S_{q2}}{\mathrm{d}t} = q_{s2} S_2 - (\eta_2 + \mu)\, S_{q2}. \end{cases} \tag{3.1}$$

A simple calculation shows that subsystem (3.1) has a unique positive equilibrium $K^* = (S_1^*, S_{q1}^*, S_w^*, S_2^*, S_{q2}^*)$ with

$$\begin{aligned} S_1^* &= \frac{\Lambda_1 (\eta_1 + \mu)}{m\eta_1 + \mu (\eta_1 + \mu + q_{s1} + m)}, \quad S_{q1}^* = \frac{\Lambda_1 q_{s1}}{m\eta_1 + \mu (\eta_1 + \mu + q_{s1} + m)}, \\ S_w^* &= \frac{\Lambda_1 m\rho (\eta_1 + \mu)}{\kappa \left[m\eta_1 + \mu (\eta_1 + \mu + q_{s1} + m)\right]}, \\ S_2^* &= \frac{\Lambda_2 (\eta_2 + \mu)}{\mu (\eta_2 + \mu + q_{s2})} + \frac{\Lambda_1 m (\eta_2 + \mu)(\eta_1 + \mu)}{\mu (\eta_2 + \mu + q_{s2}) \left[m\eta_1 + \mu (\eta_1 + \mu + q_{s1} + m)\right]}, \\ S_{q2}^* &= \frac{\Lambda_2 \mathrm{q}_{s2}}{\mu (\eta_2 + \mu + \mathrm{q}_{s2})} + \frac{\Lambda_1 m q_{s2} (\eta_1 + \mu)}{\mu (\eta_2 + \mu + q_{s2}) \left[m\eta_1 + \mu (\eta_1 + \mu + q_{s1} + m)\right]}, \end{aligned}$$

which is globally asymptotically stable. Therefore, model (2.3) has exactly a unique disease-free equilibrium $K_0 = \left(S_1^*, 0, 0, 0, S_{q1}^*, S_w^*, 0, 0, 0, S_2^*,\ 0, 0, 0, S_{q2}^*\right)$. Then, we use the next generation matrix method to calculate the basic reproduction number of model (2.3). Letting

$$F = \begin{pmatrix} 0 & c_1\beta_1 S_1^* & c_1\beta_1 S_1^* & 0 & \dots & 0 & 0 \\ 0 & 0 & 0 & 0 & \dots & 0 & 0 \\ \vdots & \vdots & \vdots & \vdots & \ddots & \vdots & \vdots \\ 0 & 0 & 0 & 0 & \dots & c_2\beta_2 S_2^* & c_2\beta_2 S_2^* \\ 0 & 0 & 0 & 0 & \dots & 0 & 0 \\ 0 & 0 & 0 & 0 & \cdots & 0 & 0 \end{pmatrix}, \ V = \begin{pmatrix} V_{11} & 0 \\ V_{21} & V_{22} \end{pmatrix},$$

where

$$V_{11} = \begin{pmatrix} \tau + \mu + q_{e1} + m & 0 & 0 \\ -\tau & \gamma_a + \sigma + \mu + q_{a1} + m & 0 \\ 0 & -\sigma & \theta_1 + \gamma + \mu + q_{i1} \end{pmatrix},$$

$$V_{21} = \begin{pmatrix} -m\rho & 0 & 0 & -m(1-\rho) & 0 & 0 \\ 0 & -m\rho & 0 & 0 & -m(1-\rho) & 0 \\ 0 & 0 & 0 & 0 & 0 & 0 \end{pmatrix}^T,$$

$$V_{22} = \begin{pmatrix} \tau_w & 0 & 0 & 0 & 0 & 0 \\ -\tau_w & \sigma_w + q_{aw} + \epsilon & 0 & 0 & 0 & 0 \\ 0 & -\sigma_w & q_{iw} & 0 & 0 & 0 \\ 0 & 0 & 0 & \tau + \mu + q_{e2} & 0 & 0 \\ 0 & -\epsilon & 0 & -\tau & \gamma_q + \sigma + \mu + q_{a2} & 0 \\ 0 & 0 & 0 & 0 & -\sigma & \theta_2 + \gamma + \mu + q_{i2} \end{pmatrix}.$$

Thus, the basic reproduction number $\bar{\mathcal{R}}_0$ of model (2.3) is given by

$$\bar{\mathcal{R}}_0 = r(FV^{-1}) = \max\left\{\bar{\mathcal{R}}_{01}, \bar{\mathcal{R}}_{02}\right\},$$

where

$$\bar{\mathcal{R}}_{01} = \frac{c_1\beta_1 S_1^*\tau\,(\theta_1 + \gamma + \mu + q_{i1} + \sigma)}{(\theta_1 + \gamma + \mu + q_{i1})\,(\gamma_a + \sigma + \mu + q_{a1} + m)\,(\tau + \mu + q_{e1} + m)},$$
$$\bar{\mathcal{R}}_{02} = \frac{c_2\beta_2 S_2^*\tau\,(\theta_2 + \gamma + \mu + q_{i2} + \sigma)}{(\theta_2 + \gamma + \mu + q_{i2})\,(\gamma_a + \sigma + \mu + q_{a2})\,(\tau + \mu + q_{e2})},$$

and $r(FV^{-1})$ is the spectral radius of matrix FV^{-1}.

Theorem 3.1. *Assume $\bar{\mathcal{R}}_0 < 1$. Then disease-free equilibrium K_0 of model* (2.3) *is locally asymptotically stable, and unstable if $\bar{\mathcal{R}}_0 > 1$.*

Moreover, based on the arguments in [24], we have the following results.

Lemma 3.2. *Let $r(F - V)$ be the principle eigenvalue of $F - V$. It is clear that $\bar{\mathcal{R}}_0 - 1$ has the same sign as $r(F - V)$.*

By calculating the characteristic equation of Jacobian matrix of model (2.3) at disease-free equilibrium K_0, we easily obtain that when $\bar{\mathcal{R}}_0 < 1$, all characteristic roots have negative real parts, and on the contrary, when $\bar{\mathcal{R}}_0 > 1$, there is a characteristic root with positive real part. Therefore, the proof of Theorem 3.1 is simple, and we here omit it.

Theorem 3.3. *Assume $\bar{\mathcal{R}}_0 < 1$. Then disease-free equilibrium K_0 of model* (2.3) *is globally asymptotically stable.*

Proof. It suffices to show that the globally attractivity of the disease-free equilibrium K_0. It follows from Theorem 3.1, we know that if $\bar{\mathcal{R}}_0 < 1$, then $r(F - V) < 0$. Then, we can choose a small enough constant $\varepsilon > 0$, such that $r(F - V + \varepsilon M) < 0$, where

$$M = \begin{pmatrix} 0 & c_1\beta_1 & c_1\beta_1 & 0 & \dots & 0 & 0 \\ 0 & 0 & 0 & 0 & \dots & 0 & 0 \\ \vdots & \vdots & \vdots & \vdots & \ddots & \vdots & \vdots \\ 0 & 0 & 0 & 0 & \dots & c_2\beta_2 & c_2\beta_2 \\ 0 & 0 & 0 & 0 & \dots & 0 & 0 \\ 0 & 0 & 0 & 0 & \cdots & 0 & 0 \end{pmatrix}.$$

From the positivity of the solution of model (2.3), we have

$$\begin{cases} \dfrac{\mathrm{d}S_1}{\mathrm{d}t} \le \Lambda_1 - (\mu + q_{s1})\, S_1 + \eta_1 S_{q1} - mS_1, \\ \dfrac{\mathrm{d}S_{q1}}{\mathrm{d}t} = q_{s1} S_1 - (\eta_1 + \mu)\, S_{q1}, \\ \dfrac{\mathrm{d}S_w}{\mathrm{d}t} = m\rho S_1 - \kappa S_w, \\ \dfrac{\mathrm{d}S_2}{\mathrm{d}t} \le \Lambda_2 + m(1-\rho) S_1 + \kappa S_w - (\mu + q_{s2})\, S_2 + \eta_2 S_{q2}, \\ \dfrac{\mathrm{d}S_{q2}}{\mathrm{d}t} = q_{s2} S_2 - (\eta_2 + \mu)\, S_{q2}. \end{cases}$$

Since the comparison system (3.1) has the positive equilibrium $K^* = (S_1^*, S_{q1}^*, S_w^*, S_2^*, S_{q2}^*)$, it is globally asymptotically stable. Hence, for above given constant $\varepsilon > 0$, there exists a $t_1 > 0$, such that for all $t > t_1$ one has $S_1(t) \le \bar{S}_1(t) < S_1^* + \varepsilon$ and $S_2(t) \le \bar{S}_2(t) < S_2^* + \varepsilon$. From model (2.3), for all $t > t_1$

$$\begin{cases} \dfrac{\mathrm{d}E_1}{\mathrm{d}t} \le c_1\beta_1 \left(S_1^* + \varepsilon\right)(I_{a1} + I_1) - (\tau + \mu + q_{e1})\, E_1 - mE_1, \\ \dfrac{\mathrm{d}I_{a1}}{\mathrm{d}t} = \tau E_1 - (\gamma_a + \sigma + \mu + q_{a1})\, I_{a1} - mI_{a1}, \\ \dfrac{\mathrm{d}I_1}{\mathrm{d}t} = \sigma I_{a1} - (\theta_1 + \gamma + \mu + q_{i1})\, I_1, \\ \dfrac{\mathrm{d}E_w}{\mathrm{d}t} = m\rho E_1 - \tau_w E_w, \\ \dfrac{\mathrm{d}I_{aw}}{\mathrm{d}t} = m\rho I_{a1} + \tau_w E_w - (\sigma_w + q_{aw} + \epsilon)\, I_{aw}, \\ \dfrac{\mathrm{d}I_w}{\mathrm{d}t} = \sigma_w I_{aw} - q_{iw} I_w, \\ \dfrac{\mathrm{d}E_2}{\mathrm{d}t} \le m(1-\rho) E_1 + c_2\beta_2 \left(S_2^* + \varepsilon\right)(I_{a2} + I_2) - (\tau + \mu + q_{e2})\, E_2, \\ \dfrac{\mathrm{d}I_{a2}}{\mathrm{d}t} = m(1-\rho) I_{a1} + \tau E_2 + \epsilon I_{aw} - (\gamma_a + \sigma + \mu + q_{a2})\, I_{a2}, \\ \dfrac{\mathrm{d}I_2}{\mathrm{d}t} = \sigma I_{a2} - (\theta_2 + \gamma + \mu + q_{i2})\, I_2. \end{cases}$$

Consider the following auxiliary system:

$$\frac{\mathrm{d}Y(t)}{\mathrm{d}t} = (F - V + \varepsilon M) Y(t), \tag{3.2}$$

where $Y(t) = \left(\bar{E}_1(t), \bar{I}_{a1}(t), \bar{I}_1(t), \bar{E}_w(t), \bar{I}_{aw}(t), \bar{I}_w(t), \bar{E}_w(t), \bar{I}_{aw}(t), \bar{I}_w(t)\right)^T$. Since $r(F - V + \varepsilon M) < 0$, all eigenvalues of $F - V + \varepsilon M$ are with negative real parts. Hence, all non-negative solutions of system (3.2) satisfy $\lim_{t\to\infty} Y(t) = 0$. By a standard comparison principle, we conclude that if $\bar{\mathcal{R}}_0 < 1$, then all non-negative solutions of model (2.3) satisfy $\lim_{t\to\infty} E_i(t) = 0$, $\lim_{t\to\infty} I_{ai}(t) = 0$ and $\lim_{t\to\infty} I_i(t) = 0$, for $i = 1, 2, w$. Moreover, from the equations of $S_1(t)$, $S_{q1}(t)$, $S_w(t)$, $S_2(t)$ and $S_{q2}(t)$ in model (2.3), we can get

$$\lim_{t\to\infty} (S_1(t), S_{q1}(t), S_w(t), S_2(t), S_{q2}(t)) = (S_1^*, S_{q1}^*, S_w^*, S_2^*, S_{q2}^*).$$

Consequently, we deduce that disease-free equilibrium K_0 of model (2.3) is globally attractive when $\bar{\mathcal{R}}_0 < 1$. This completes the proof. □

Remark 3.1. From the expression of $\mathcal{R}_{02}$ and $\bar{\mathcal{R}}_{02}$, we can obtain

$$\bar{\mathcal{R}}_{02} = \mathcal{R}_{02} + \frac{c_2\beta_2\tau\Lambda_1 m(\eta_2+\mu)(\eta_1+\mu)(\theta_2+\gamma+\mu+q_{i2}+\sigma)}{\mu(\eta_2+\mu+q_{s2})[m\eta_1+\mu(\eta_1+\mu+q_{s1}+m)]\Upsilon},$$

where $\Upsilon = (\theta_2+\gamma+\mu+q_{i2})(\gamma_a+\sigma+\mu+q_{a2})(\tau+\mu+q_{e2})$. It is easy to see that, once the border is reopened, the infection risk of people in patch-2 will increase, and the basic reproduction number of patch-2 may change from less than 1 to more than 1. In other words, a reopen border may cause a disease state from extinction to endemic in patch-2. Therefore, the extent of border reopening (value of m) is crucial to the transmission of disease in patch-2. Once the value of m makes $\bar{\mathcal{R}}_{02}$ greater than 1, patch-2 may need to consider closing the border again.

A simple calculation shows that if $\bar{\mathcal{R}}_{01} < 1$ and $\bar{\mathcal{R}}_{02} > 1$, then model (2.3) exists as the patch-1 disease-free and patch-2 endemic boundary equilibrium $K_2 = (\tilde{S}_1, 0, 0, 0, \tilde{S}_{q1}, \tilde{S}_w, 0, 0, 0, \tilde{S}_2, \tilde{E}_2, \tilde{I}_{a2}, \tilde{I}_2, \tilde{S}_{q2})$, where

$$\begin{aligned}
&\tilde{S}_1 = S_1^*,\ \tilde{S}_{q1} = S_{q1}^*,\ \tilde{S}_w = S_w^*, \quad \tilde{S}_2 = \frac{S_2^*}{\bar{\mathcal{R}}_{02}},\ \tilde{S}_{q2} = \frac{\mathrm{q}_{s2}S_2^*}{\bar{\mathcal{R}}_{02}(\eta_2+\mu)},\\
&\tilde{E}_2 = \frac{\mu(\theta_2+\gamma+\mu+q_{i2})(\gamma_a+\sigma+\mu+q_{a2})(\eta_2+\mu+q_{s2})(\bar{\mathcal{R}}_{02}-1)}{c_2\beta_2\tau(\eta_2+\mu)(\theta_2+\gamma+\mu+q_{i2}+\sigma)},\\
&\tilde{I}_{a2} = \frac{\mu(\theta_2+\gamma+\mu+q_{i2})(\eta_2+\mu+q_{s2})(\bar{\mathcal{R}}_{02}-1)}{c_2\beta_2\tau(\eta_2+\mu)(\theta_2+\gamma+\mu+q_{i2}+\sigma)},\\
&\tilde{I}_2 = \frac{\mu\sigma(\eta_2+\mu+q_{s2})(\bar{\mathcal{R}}_{02}-1)}{c_2\beta_2\tau(\eta_2+\mu)(\theta_2+\gamma+\mu+q_{i2}+\sigma)}.
\end{aligned}$$

Theorem 3.4. *Assume $\bar{\mathcal{R}}_{01} < 1$ and $\bar{\mathcal{R}}_{02} > 1$. Then the patch-1 disease-free and patch-2 endemic boundary equilibrium K_2 of model* (2.3) *is locally asymptotically stable.*

Theorem 3.4 can be easily proved by calculating the characteristic equation of Jacobian matrix of model (2.3) at boundary equilibrium K_2, and then verified that all characteristic roots have the negative real parts. We hence omit it here.

Remark 3.2. When $\bar{\mathcal{R}}_{01} < 1, \bar{\mathcal{R}}_{02} > 1$, then the disease will be endemic in patch-2, but extinct in patch-1. That is to say, in model (2.3), the basic reproduction number $\bar{\mathcal{R}}_0$ greater than 1 does not necessarily lead to persistent disease epidemics throughout the system.

Theorem 3.5. *If $\bar{\mathcal{R}}_{01} > 1$, then model* (2.3) *has a unique endemic equilibrium.*

Theorem 3.5 can be easily proved by directly solving the equation of endemic equilibrium K_3 =

$(\hat{S}_1, \hat{E}_1, \hat{I}_{a1}, \hat{I}_1, \hat{S}_{q1}, \hat{S}_w, \hat{E}_w, \hat{I}_{aw}, \hat{I}_w, \hat{S}_2, \hat{E}_2, \hat{I}_{a2}, \hat{I}_2, \hat{S}_{q2})$ as follows

$$\begin{cases} \Lambda_1 - c_1\beta_1\hat{S}_1(\hat{I}_{a1} + \hat{I}_1) - (\mu + q_{s1} + m)\hat{S}_1 + \eta_1\hat{S}_{q1} = 0, \\ c_1\beta_1\hat{S}_1(\hat{I}_{a1} + \hat{I}_1) = (\tau + \mu + q_{e1} + m)\hat{E}_1, \\ \tau\hat{E}_1 = (\gamma_a + \sigma + \mu + q_{a1} + m)\hat{I}_{a1}, \\ \sigma\hat{I}_{a1} = (\theta_1 + \gamma + \mu + q_{i1})\hat{I}_1, \quad q_{s1}\hat{S}_1 = (\eta_1 + \mu)\hat{S}_{q1}, \\ \rho\hat{S}_1 = \kappa\hat{S}_w, \quad m\rho\hat{E}_1 = \tau_w\hat{E}_w, \\ m\rho\hat{I}_{a1} + \tau_w\hat{E}_w = (\sigma_w + q_{aw} + \varepsilon)\hat{I}_{aw}, \quad \sigma_w\hat{I}_{aw} = q_{iw}\hat{I}_w, \\ \Lambda_2 + m(1-\rho)\hat{S}_1 + \kappa\hat{S}_w - c_2\beta_2\hat{S}_2(\hat{I}_{a2} + \hat{I}_2) - (\mu + q_{s2})\hat{S}_2 + \eta_2\hat{S}_{q2} = 0, \\ m(1-\rho)\hat{E}_1 + c_2\beta_2\hat{S}_2(\hat{I}_{a2} + \hat{I}_2) = (\tau + \mu + q_{e2})\hat{E}_2, \\ m(1-\rho)\hat{I}_{a1} + \tau\widehat{E_2} + \varepsilon\hat{I}_{aw} = (\gamma_a + \sigma + \mu + q_{a2})\hat{I}_{a2}, \\ \sigma\hat{I}_{a2} = (\theta_2 + \gamma + \mu + q_{i2})\hat{I}_2, \quad q_{s2}\hat{S}_2 = (\eta_2 + \mu)\hat{S}_{q2}. \end{cases}$$

We here omit it.

Following the expression of $\mathcal{R}_{01}$ and $\bar{\mathcal{R}}_{01}$, we obtain $\bar{\mathcal{R}}_{01} = \mathcal{R}_{01}\bar{\mathcal{R}}^m_{01}$, where

$$\bar{\mathcal{R}}^m_{01} = \frac{\gamma_a + \sigma + q_{a1} + \mu}{\gamma_a + \sigma + q_{a1} + \mu + m} \times \frac{\tau + q_{e1} + \mu}{\tau + q_{e1} + \mu + m} \times \frac{\mu(\eta_1 + q_{s1} + \mu)}{m\eta_1 + \mu(\eta_1 + q_{s1} + \mu + m)}.$$

Remark 3.3. It can be seen from Theorem 3.5 that, if the border is reopened under the condition of $\mathcal{R}_{01} > 1/\bar{\mathcal{R}}^m_{01}$, the disease will be prevalent in patch-1 and patch-2, and eventually become co-existence endemic in the two patches. Therefore, in order to prevent this situation, it is better to allow people in patch-1 to enter into patch-2 under $\mathcal{R}_{01} < 1/\bar{\mathcal{R}}^m_{01}$.

4. Numerical simulation

While several reliable vaccines have been developed for COVID-19, as far as we know, no vaccine is 100% effective, that is to say that, there is still a risk of infection with novel coronavirus after vaccination [25]. Moreover, there is no specific medicine for COVID-19. Hence, the relevant NPIs policies on COVID-19 are still preferred approaches in all countries, such as keeping masks, keep social distance, and the strict border control strategies among countries and so on. In this section, we do some simulations to investigate the impact of relevant local (for one patch) NPIs policies on COVID-19 transmission and control, as well as the impact of border control strategies between two patches on local disease transmission. The possible values of parameters for model (2.1) and model (2.3) are listed in Table 1, and we fix some basic model parameters as follows: $\Lambda_1 = 695$, $\Lambda_2 = 449$, $\mu = 1/(78 * 365)$, $\eta_1 = \eta_2 = 1/14$, $\tau = 1/4$, $\gamma_a = 1/14$, $\sigma = 0.327$, $\gamma = 1/15$, $\theta_1 = \theta_2 = 0.0152$, $\delta_1 = \delta_2 = 0.02$, $\gamma_{q1} = \gamma_{q2} = 1/8$, $\gamma_{h1} = \gamma_{h2} = 1/15$, $d_1 = 0.00012$, $d_2 = 0.0001$, $\kappa = 1/14$, $\tau_w = 1/3$, $\sigma_w = 0.3$.

The basic reproduction number $\mathcal{R}_0$ is a significant indicator to measure the risk of disease transmission and how to develop control measures. In order to provide a comprehensive understanding of the influence of different local NPIs policies on COVID-19 transmission and control, the sensitivity analysis is conducted by obtaining the partial rank correlation coefficients (PRCCs) for various parameters against $\mathcal{R}_0$. In the case of border close, we study the influence of the relevant local (for only one patch

case) NPIs policies on the the basic reproduction number $\mathcal{R}_0$. Without loss of generality, here, we take patch-2. Give two groups of different parameter ranges for patch-2 in Table 2. The Group I represents the initial stage of the disease in which all kinds of control measures are not mature and the tracking ability is limited. Group II implies not only to maintain social distance and wear masks, but also to strengthen tracking for all carriers of the virus, and even increase the duration of quarantine for those who are traced to be susceptible (the change of η).

Table 2. Definition and possible values of the basic parameter for model (2.3)

Param.	Group I	Group II
β_2	$(2.0\times10^{-9}, 3.5\times10^{-9})$	$(1.0\times10^{-9}, 2.0\times10^{-9})$
c_2	(8,14)	(5,8)
q_{s2}	(0.0.001)	(0,0.01)
q_{e2}	(0,0.1)	(0.2,0.9)
q_{a2}	(0,0.1)	(0.2,0.7)
q_{i2}	(0,0.3)	(0.4,1)
η_2	(1/14,1/7)	(1/28,1/14)

Figure 3 (a) and (b) illustrates the PRCCs of $\mathcal{R}_{02}$ with respect to parameters Group I and Group II, respectively. Figure 3(a) implies that the basic reproduction number $\mathcal{R}_{02}$ is the most sensitive to the forced quarantine rate of symptomatic infected, followed by the contact rate and transmission rate, followed by the quarantine rates of exposed and subclinical infected individuals, and finally, the quarantine rate and quarantine time of susceptible individuals. Figure 3 (b) indicates that the basic reproduction number $\mathcal{R}_{02}$ is the most sensitive to the quarantine rate of exposed individuals, followed by the contact rate and transmission rate, followed by the quarantine rate of subclinical infected individuals and the forced quarantine rate of symptomatic infected individuals, and finally, the quarantine rate and quarantine time of susceptible individuals. Comparing Figure 3 (a) and (b), we find that the sensitivity of the quarantine rate of exposed person and the forced quarantine rate of symptomatic infected changes under different intensities of NPIs policies. At the same time, in either case, the contact rate and transmission rate are always relative sensitive for the basic reproduction number $\mathcal{R}_{02}$. Moreover, the sensitivity of $\mathcal{R}_{02}$ with respect to the quarantine rate and lengthening the quarantine time of susceptible individuals significantly changes under different intensities of NPIs policies. Biologically, appropriate intensities of NPIs policies can be effective in controlling the risk of disease transmission.

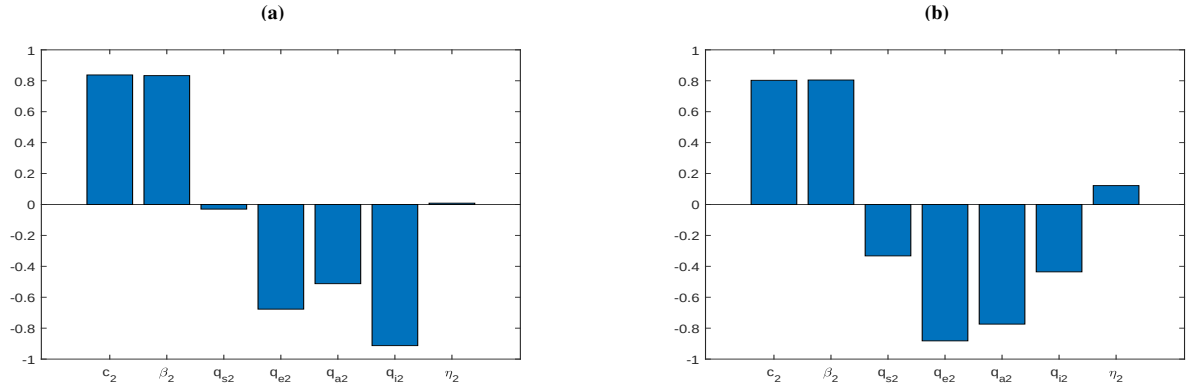

Figure 3. PRCCs of $\mathcal{R}_{02}$ with respect to model parameters.

Next, we investigate the degree of effect of the border open (the value of m corresponds to the degree of border opening) between the two patches on the transmission and control of COVID-19. To this end, we carry out numerical simulation analysis from two aspects. First, when the basic reproduction number $\mathcal{R}_{02}$ of the patch-2 is less than 1, we open the border to study the influence of the open border on the epidemic of patch-2. Second, in the case of open border, we study the effect of the degree of the border open on the epidemic of patch-2 by adjusting the move rate m of people between the two patches. For model (2.1), we set $c_1 = c_2 = 10$, $\beta_1 = 1.8034 \times 10^{-9}$, $\beta_2 = 3.0 \times 10^{-9}$, $q_{s1} = 0.00002$, $q_{s2} = 0.0004$, $q_{e1} = 0.1$, $q_{e2} = 0.2$, $q_{a1} = 0.15$, $q_{a2} = 0.1$ and $q_{i1} = q_{i2} = 0.3$ and compute the corresponding basic reproduction numbers $\mathcal{R}_{01} = 0.8624$ and $\mathcal{R}_{02} = 0.7891$. Thus, the disease goes extinct in patch-1 and patch-2 if the border remains closed. In this case, we open the border between the two patches, and mathematically, there are some new parameters introduced and the model (2.1) of patch-2 changes to (2.3). Let $m = 0.001$, $\rho = 0.8$, $\epsilon = 0.05$, $q_{aw} = 0.01$ and $q_{iw} = 0.1$, we can easily find the basic reproduction number of patch-2 changing from less than 1($\mathcal{R}_{02} = 0.7891$ for model (2.1)) to greater than 1($\bar{\mathcal{R}}_{02} = 1.9690$ for model (2.3)), that is to say, the disease of patch-2 changes from extinction to outbreak. Figure 4(a) gives an intuitive description of the numerical simulation results, and the above implies the case of border close, the corresponding $\mathcal{R}_{02} = 0.7891 < 1$ and the disease is extinct. However, the bottom one indicates the $\bar{\mathcal{R}}_{02} = 1.9690 > 1$ when the border opens and there is an outbreak of disease, and even a second outbreak two or three years later. Figure 4(b) shows that the number of symptomatic infected in patch-2 increases with the increase of move rate m, and the time to reach the peak also moves forward, which is to say that the adjustment of degree of the border open has a significant influence on the epidemic of patch-2.

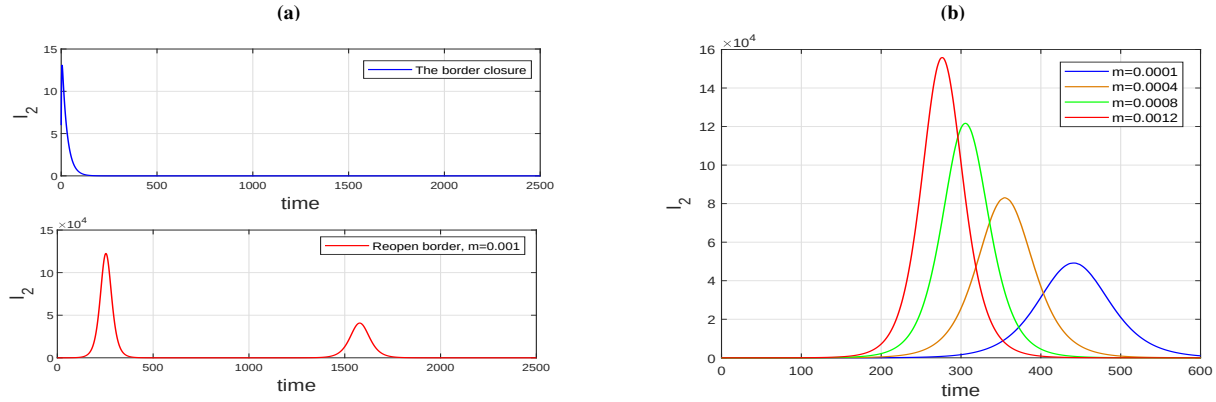

Figure 4. The effect of move rate m.

Then, choose $c_1 = c_2 = 10$, $\beta_1 = 1.8034 \times 10^{-9}$, $\beta_2 = 2.5 \times 10^{-9}$, $q_{s1} = 0.00002$ $q_{s2} = 0.00004$, $q_{e1} = q_{e2} = 0.1$, $q_{a1} = 0.15$, $q_{a2} = 0.1$, $q_{i1} = q_{i2} = 0.3$, $m = 0.001$, $\epsilon = 0.05$, $q_{aw} = 0.01$ and $q_{iw} = 0.1$. We conduct some numerical simulations to investigate the impact of border control measures and local NPIs polices on local outbreaks. To this end, we first give one special initial value for model (2.3) $(1.3 \times 10^7, 1040, 1020, 510, 5, 0, 0, 0, 1.9 \times 10^7, 0, 0, 0, 0)$, that is to say patch-2 has no epidemic in the initial state. Based on discussion above, we know the fact that the disease will cause an outbreak if the border opens without strict enough NPIs polices. But, there is a fact that, if patch-2 has no epidemic in the initial state, even if we open the border, as long as our border control measures are strict enough, there will be no disease outbreak in patch-2. The blue line of Figure 5 (a) shows that if the border

concentrated quarantine places can check out all of subclinical disease, namely the miss rate $\epsilon = 0$, and the ability to do give all people conventional entry with centralized quarantine, namely $\rho = 1$, the number of daily new infectious equals to zero, the disease will not cause outbreak in patch-2. In fact, once the carriers of the virus are detected, they will be quarantined and sent to hospitals immediately at the border centralized quarantine places, and will not transfer the virus to the local population, and then will not cause the disease outbreak. However, the red line of Figure 5 (a) shows that if $\epsilon = 0$ and $\rho = 0.99$, the disease will be prevalent in patch-2. Biologically, a small enough percentage of unconventional arrivals will cause the disease epidemic. Then, we fix parameter $\epsilon = 0.05$, and discuss the effect of different degrees of conventional entry on the disease transmission, i.e., take $\rho = 0.1, 0.4, 0.7$ and 1, respectively, we obtain the Figure 5 (b) and (c). These two figures imply that, although ρ does not appear in the expression of the basic regeneration number $\bar{\mathcal{R}}_0$, that is, the value of ρ does not affect the final state (epidemic or extinction) of the disease in the two patches, the value of ρ affects the number of infected in patch-2 in a short time. Specifically, the larger the value of ρ (the stricter the control), the slower the growth of number of new infectious in patch-2.

Moreover, by means of numerical calculation, we also discuss the relationship among the basic reproduction number $\bar{\mathcal{R}}_0$, the proportion of conventional entry ρ and transmission rate β_2. Because ρ does not exist in the expression of the basic reproduction number $\bar{\mathcal{R}}_0$ for model (2.3), here, we define an instantaneous risk index of model (2.3) by ideas from Refs. [26–29] as follows,

$$\bar{\mathcal{R}}_0(t) = \max\left\{\bar{\mathcal{R}}_{01}(t), \bar{\mathcal{R}}_{02}(t)\right\}$$

where

$$\bar{\mathcal{R}}_{01}(t) = \frac{c_1\beta_1 S_1(t)\tau\,(\theta_1 + \gamma + \mu + q_{i1} + \sigma)}{(\theta_1 + \gamma + \mu + q_{i1})\,(\gamma_a + \sigma + \mu + q_{a1} + m)\,(\tau + \mu + q_{e1} + m)},$$

$$\bar{\mathcal{R}}_{02}(t) = \frac{c_2\beta_2 S_2(t)\tau\,(\theta_2 + \gamma + \mu + q_{i2} + \sigma)}{(\theta_2 + \gamma + \mu + q_{i2})\,(\gamma_a + \sigma + \mu + q_{a2})\,(\tau + \mu + q_{e2})},$$

where $S_1(t)$ and $S_2(t)$ satisfies model (2.3). Numerically, we obtain the Figure 5(d) and Figure 5(e). From the intuition of the these two graphs, we can see that as ρ decreases (the proportion of conventional arrivals decreases), so does the transmission rate in order to reduce the instantaneous risk index for patch-2. Biologically, after the opening of the border, in order to avoid increasing the transmission risk of local diseases, we should start from the following two aspects: first, strengthen the border control measures (for example, isolate all the immigrants and ensure no missing detection); second, strengthen the intensity of local NPIs polices (such as requiring local people to wear masks, maintain social distance and increase tracking intensity).

Similarly, select the same initial values and parameter values as in Figure 5, where we conduct some numerical simulations to investigate the impact of the rate of subclinical infections not detected at the border quarantine on local disease transmission. The blue line of Figure 6 (a) shows that if the border concentrated quarantine places can check out all subclinical diseases, i.e. $\epsilon = 0$, and the ability to do all entries as conventional, then entries are centralized quarantine, namely $\rho = 1$, the number of daily new infectious equals to zero, the disease will not cause an outbreak in patch-2. However, the red line of Figure 6(a) shows that if $\epsilon = 0.05$ and $\rho = 1$, the disease will be prevalent in patch-2. Biologically, a small enough percentage of virus carrier input to the local system will cause the disease epidemic in patch-2. Fixed parameter $\rho = 0.8$, and ϵ was selected to be equal to 0.05, 0.1, 0.15 and 0.2, respectively. The simulation results are shown in Figure 6(b) and Figure 6(c), indicating that when there are already

COVID-19 cases in patch-2, the percentage of missing detection of subclinical infected at the border quarantine places has a very weak influence on the number of infected individuals in patch-2.

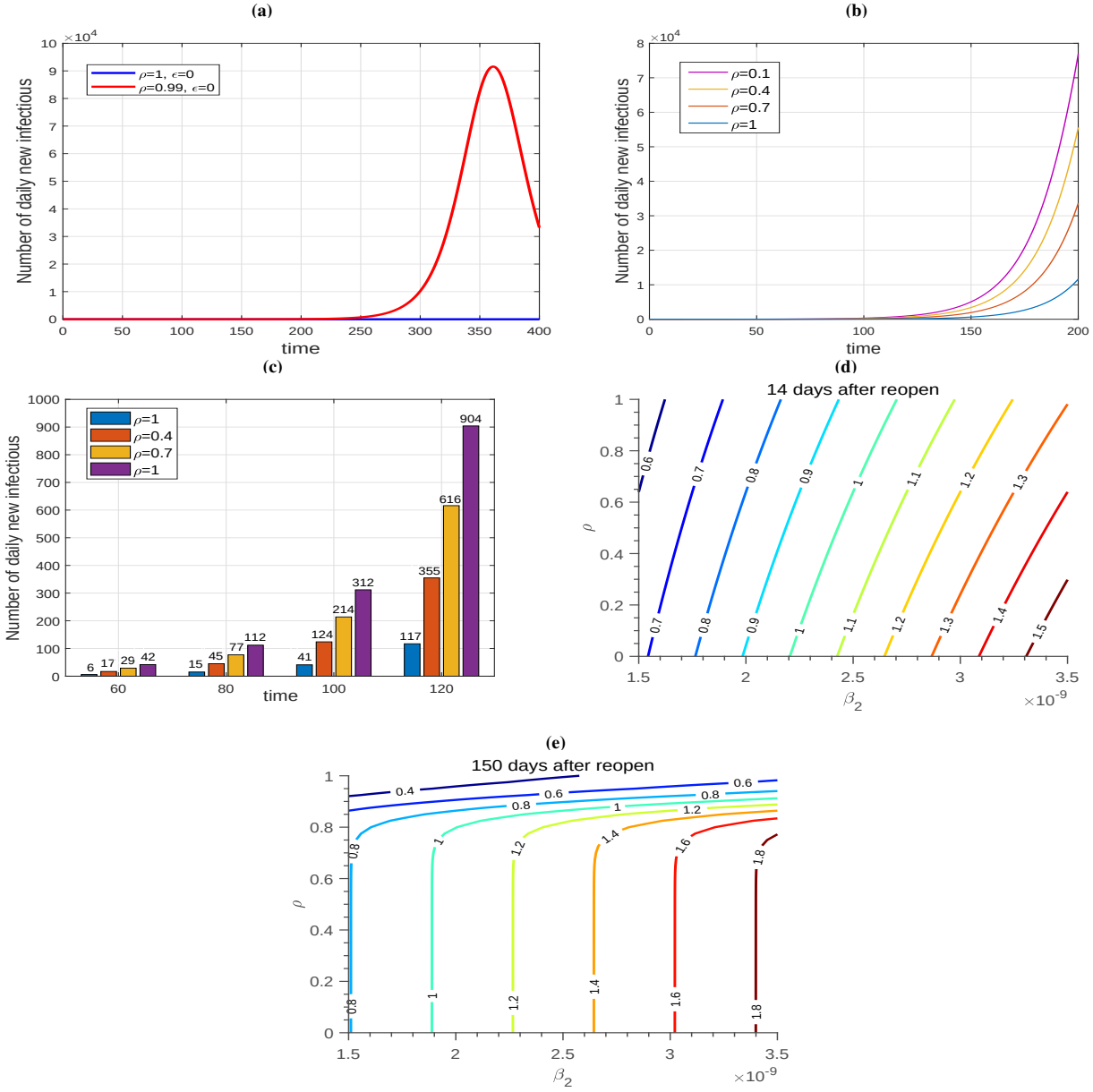

Figure 5. The effect of the rate of conventional entry individuals ρ.

Finally, it can be concluded from Figure 5 and Figure 6 that when there are no unquarantine cases of COVID-19 in patch-2, strict quarantine control measures and accurate detection technology at entry centralized quarantine places can prevent the epidemic in patch-2. However, once COVID-19 cases are introduced in patch-2, the disease will be prevalent in patch-2. That is to say that the impact of the intensity of border quarantine control on the transmission of the disease is not obvious when there are already COVID-19 cases in patch-2. In this case, to achieve open borders without increasing the risk of disease, it is necessary to strengthen the prevention and control measures in patch-2, such as

increasing the proportion of masks worn, reducing social contact, closing public places, increasing the rate of tracking and quarantine and mandatory quarantine for symptomatic patients. Therefore, we draw the counter plots of $\bar{\mathcal{R}}_{02}$ with m and parameters β_2, c_2, q_{e2}, q_{a2} and q_{i2}, respectively, as shown in Figure 7. Specifically, it can be seen from Figure 7(a) that fixed $\beta_2 = 3.0 \times 10^{-9}$, and the basic reproduction number of patch-2 will soon become greater than a unit with the increase of m. Fixed $m = 0.00006, \beta_2$ can only be reduced from 3.0×10^{-9} to about 1.5×10^{-9}, so that the basic reproduction number is no higher than before the border opening ($m = 0, \mathcal{R}_{02} = 0.7891$), c_2 is similar to β_2. Fixed $q_{e2} = 0.2$, and the basic reproduction number of patch-2 will soon become greater than a unit with the increase of m and fixed $m = 0.00006$, q_{e2} can only be increased from 0.2 to about 0.6, so that the basic reproduction number is no higher than before the border opening ($m = 0, \mathcal{R}_{02} = 0.7891$). The basic reproduction number has a similar trend with m-q_{e2}, m-q_{a2} and m-q_{i2}. It is worth mentioning that Figure 7(e) shows that when $m > 0.0006$, only increasing the value of q_{i2} cannot reduce the value of the basic reproduction number to less than 1. Hence, after the border is opened, patch-2 must simultaneously increase the strength of various control measures to ensure that the local disease risk is not increased. Therefore, during the epidemic period, there is a great risk for low-risk areas to open the border to high-risk areas.

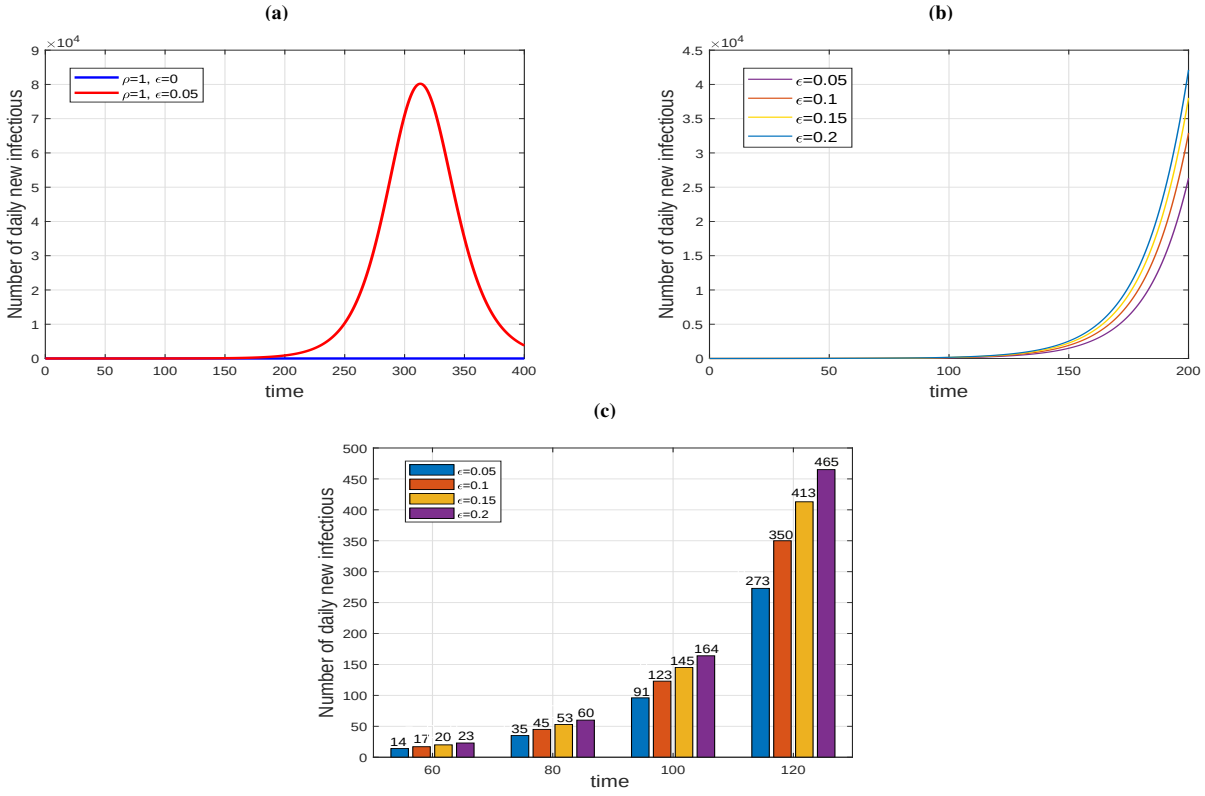

Figure 6. The effect of the rate of subclinical infections that are not detected at the border quarantine ϵ.

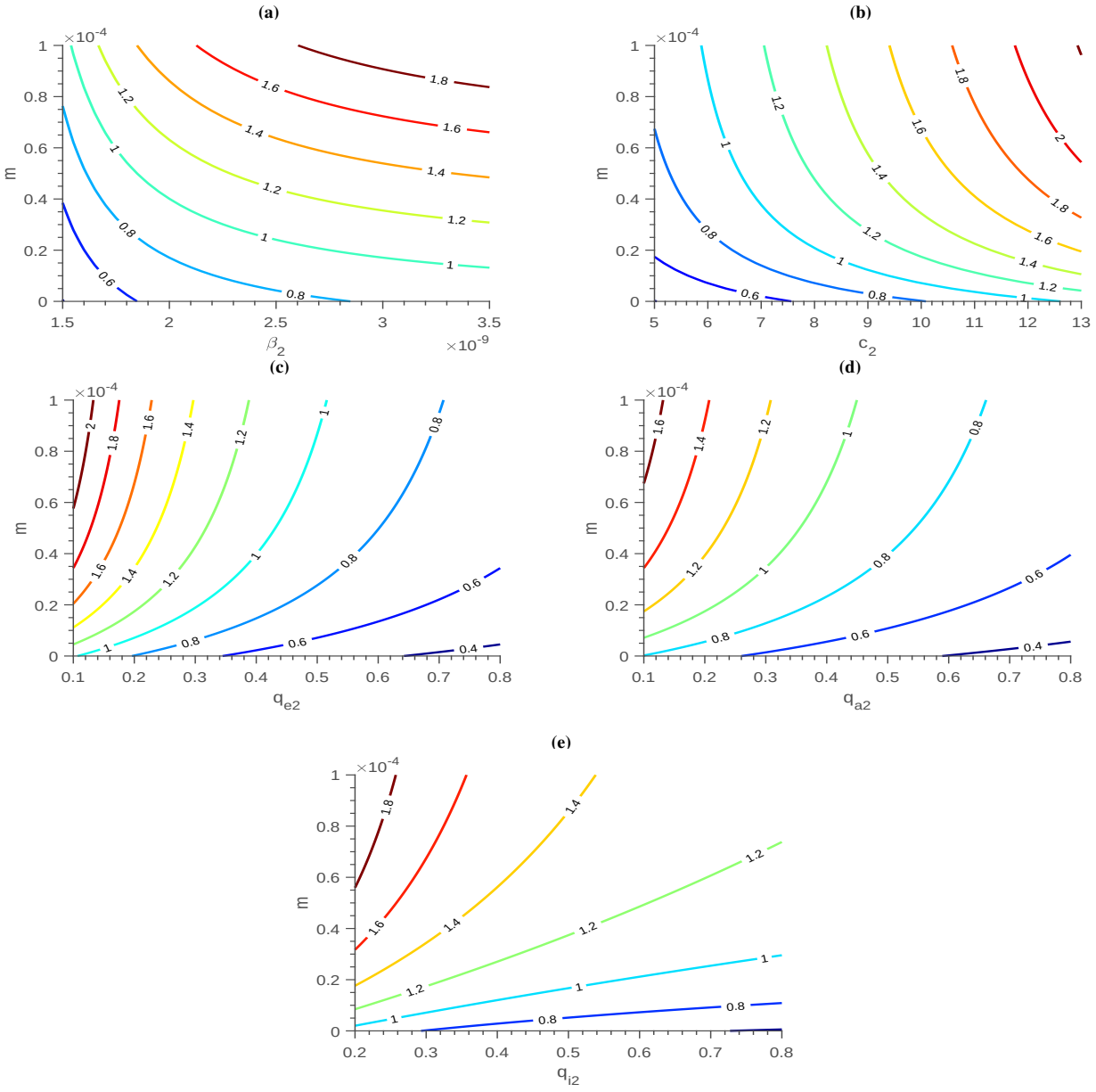

Figure 7. The contour plot of the reproduction number $\bar{\mathcal{R}}_{02}$ under four different scenarios. The x-axes represent the relative frequency exchange rates β_2, c_2, q_{e2}, q_{i2} and q_{i2}, respectively, and y-axes represent the relative frequency exchange rate m.

5. Discussion

In this paper, we propose a two-patch COVID-19 model with border control measures to quantitatively analyze whether liberalization can be implemented, and what measures should be taken to avoid the recurrence of epidemic in local areas after liberalization. The dynamics of each patch in the cases of border closure are described in terms of the basic reproduction number $\mathcal{R}_{0j}$. When the basic reproduction number of patch-2 is less than 1, we consider the reopening of the border between patch-2 and patch-1, and propose a two-patch model (2.3) with border control. In model (2.3), patch-2 allows peo-

ple in patch-1 to enter, and central quarantine measures are implemented at the border of patch-2. We calculate the basic reproduction number of model (2.3), and obtain the existence of various boundary equilibria and the existence of coexistence equilibrium of model (2.3).

In numerical simulations, we focus on verifying the impact of various NPIs policies on local containment under border closure, and the influence of the degree of border reopening, the intensity of border control and the possibility of missing detection of subclinical infected individuals at the border quarantine on the transmission and control of the disease in patch-2 after the reopening of the border. For the convenience of calculation and theoretical analysis, in this paper, we only consider the two-patch model that moves in one direction from patch-1 to patch-2. Therefore, we are focusing on the impact of imported people on the transmission of the disease in patch-2 after reopening the border. Theoretical results show that after the outbreak of patch-2 is under control, reopening the border may also lead to another outbreak of patch-2. In the numerical simulation, Figure 4 verifies this result. On the other hand, Figure 5(a) and Figure 6(a) show that if the border is reopened after the unquarantined virus carriers ($E_2(t), I_{a2}(t), I_2(t)$) in patch-2 are cleared, and there are no unconventional entry and missed detection (the border control is very strict), no new infections will occur locally in patch-2, that is, the disease will never be prevalent in patch-2. Numerical simulation results show that once infected individuals flow into the unquarantine system in patch-2, the intensity of border control and the size of the missed detection rate will not change the result of whether the disease is prevalent in patch-2 or not. Therefore, the control of the epidemic in patch-2 still depends on strengthening the local NPIs policy of patch-2.

Acknowledgement

This research was supported by the Natural Science Foundation of Xinjiang (Grant No. 2022D01C699, 2022D01C64) and the National Natural Science Foundation of China (Grant Nos. 11961071, 12061079, 12101529, 12201540), and the China Scholarship Council under a joint-training program at York University.

Conflict of interest

We declare there is no conflict of interest.

References

1. COVID-19 Coronavirus Pandemic. Available from: https://www.worldometers.info/coronavirus
2. Coronavirus disease (COVID-19): Vaccines. Available from: https://www.who.int/news-room/questions-and-answers/item/coronavirus-disease-(covid-19)-vaccines
3. J. Seungpil, K. Jong-Hoon, H. Seung-Sik, C. Junyoung, L. Woojoo, Modified susceptible-exposed-infectious-recovered model for assessing the effectiveness of non-pharmaceutical interventions during the COVID-19 pandemic in Seoul, *J. Theor. Biol.*, **557** (2023), 111329. https://doi.org/10.1016/j.jtbi.2022.111329

4. M. Chinazzi, J. T. Davis, M. Ajelli, C. Gioannini, M. Litvinova, S. Merler, et al., The effect of travel restrictions on the spread of the 2019 novel coronavirus (COVID-19) outbreak, *Science*, **368** (2020), 395–400. https://doi.org/10.1126/science.aba9757

5. S. Chang, E. Pierson, P. W. Koh, J. Gerardin, B. Redbird, D. Grusky, et al., Mobility network models of COVID-19 explain inequities and inform reopening, *Nature*, **589** (2021), 82–87. https://doi.org/10.1038/s41586-020-2923-3

6. K. Ousmane, D. Abou Bakari, S. Boureima, Mathematical analysis of the impact of the media coverage in mitigating the outbreak of COVID-19, *Math. Comput. Simul.*, **205** (2023), 600–618. https://doi.org/10.1016/j.matcom.2022.10.017

7. H. Tu, X. Wang, S. Tang, Exploring COVID-19 transmission patterns and key factors during epidemics caused by three major strains in Asia, *J. Theor. Biol.*, **557** (2023), 111336. https://doi.org/10.1016/j.jtbi.2022.111336

8. Z. Yang, Z. Zeng, K. Wang, S. S. Wong, W. Liang, M. Zanin, et al., Modified SEIR and AI prediction of the epidemics trend of COVID-19 in China under public health interventions, *J. Thoracic Dis.*, **12** (2020), 165–174. https://doi.org/10.21037/jtd.2020.02.64

9. D. Glass, European and US lockdowns and second waves during the COVID-19 pandemic, *Math. Biosci.*, **330** (2020), 108472. https://doi.org/10.1016/j.mbs.2020.108472

10. X. Sun, Y. Xiao, X. Ji, When to lift the lockdown in Hubei province during COVID-19 epidemic? An insight from a patch model and multiple source data, *J. Theor. Biol.*, **507** (2020), 110469. https://doi.org/10.1016/j.jtbi.2020.110469

11. L. Hu, S. Wang, T. Zheng, Z. Hu, Y. Kang, L. Nie, et al., The effects of migration and limited medical resources of the transmission of SARS-CoV-2 model with two patches, *Bull. Math. Biol.*, **84** (2022), 55. https://doi.org/10.1007/s11538-022-01010-w

12. L. Zou, S. Ruan, A patch model of COVID-19: The effects of containment on Chongqing, *Acta Math. Appl. Sin.*, **43** (2020), 310–323. https://doi.org/10.12387/C2020025

13. S. Zhao , C. T. Bauch, D. H. He, Strategic decision making about travel during disease outbreaks: A game theoretical approach, *J. R. Soc. Interface*, **15** (2020), 20180515. http://dx.doi.org/10.1098/rsif.2018.0515

14. R. S. Quilliam, P. Cross, A. P. Williams, G. Edwards-Jones, R. L. Salmon, et al., Subclinical infection and asymptomatic carriage of gastrointestinal zoonoses: Occupational exposure, environmental pathways, and the anonymous spread of disease, *Epidemiol. Infect.*, **141** (2013), 2011-2021. https://doi.org/10.1017/S0950268813001131

15. B. Tang, F. Xia, S. Tang, L. B. Nicola, Q. Li, X. Sun, et al., The effectiveness of quarantine and isolation determine the trend of the COVID-19 epidemic in the final phase of the current outbreak in China, *Int. J. Infect. Dis.*, **96** (2020), 636–647. https://doi.org/10.1016/j.ijid.2020.05.113

16. P. Yuan, J. Li, E. Aruffo, E. Gatov, Q. Li, T. Zheng, et al., Efficacy of 'Stay-at-Home' Policy and Transmission of COVID-19 in Toronto, Canada: A Mathematical Modeling Study, *CMAJ OPEN*, **10** (2022), E367–E378. https://doi.org/10.9778/cmajo.20200242

17. J. Li, P. Yuan, J. Heffernan, T. Zheng, N. Ogden, B. Sander, et al., Observation wards and

control of the transmission of COVID-19 in Wuhan, *Bull. World Health Organ.*, **98** (2020). http://dx.doi.org/10.2471/BLT.20.258152

18. X. Wang, H. Wu, S. Tang, Assessing age-specific vaccination strategies and post-vaccination re-opening policies for COVID-19 control using SEIR modeling approach, *Bull. Math. Biol.*, **84** (2022), 108. https://doi.org/10.1007/s11538-022-01064-w
19. Y. Luo, L. Zhang, Z. Teng, D.L. DeAngelis, A parasitism-mutualism-predation model consisting of crows, cuckoos and cats with stage-structure and maturation delays on crows and cuckoos, *J. Theor. Biol.*, **446** (2018), 212–228. https://doi.org/10.1016/j.jtbi.2018.02.028
20. D. Gao, How does dispersal affect the infection size, *SIAM J. Appl. Math.*, **80** (2020), 2144–2169. https://doi.org/10.1137/19M130652X
21. L. Liu, D. Jiang, T. Hayat, Dynamics of an SIR epidemic model with varying population sizes and regime switching in a two patch setting, *Phys. A*, **574** (2021), 125992. https://doi.org/10.1016/j.physa.2021.125992
22. D. Yan, X. Zou, Dynamics of an epidemic model with relapse over a two-patch environment, *Math. Biosci. Eng.*, **17** (2020), 6098–6127. https://doi.org/10.3934/mbe.2020324
23. J. Zhang, C. Cosner, H. Zhu, Two-patch model for the spread of West Nile virus, *Bull. Math. Biol.*, **80** (2018), 840–863. https://doi.org/10.1007/s11538-018-0404-8
24. Y. Luo, S. Tang, Z. Teng, L. Zhang, Global dynamics in a reaction-diffusion multi-group SIR epidemic model with nonlinear incidence, *Nonlinear Anal-Real.*, **50** (2019), 365–385. https://doi.org/10.1016/j.nonrwa.2019.05.008
25. N. Firouzabadi, P. Ghasemiyeh, S. Mohammadi-Samani, A focused review on technologies, mechanisms, safety, and efficacy of available COVID-19 vaccines, *Int. Immunopharmacol.*, **100** (2021), 108162. https://doi.org/10.1016/j.intimp.2021.108162
26. F. Brauer, C. Castillo-Chavez, *Mathematical Models in Population Biology and Epidemics*, Springer-Verlag, New York, 2000. https://doi.org/10.1007/978-1-4757-3516-1
27. S. Busenberg, K. Cooke, *Vertically Transmitted Diseases*, *Springer-Verlag*, New York, 1993. https://doi.org/10.1016/B978-0-12-434170-8.50029-7
28. J. M. Heffernan, R. J. Smith, L. M. Wahl, Perspectives on the basic reproductive ratio, *J. R. Soc. Interface*, **2** (2005), 281–293. https://doi.org/10.1098/rsif.2005.0042
29. G. F. Webb, M. J. Blaser, H. Zhu, S. Ardal, J. Wu, Critical role of nosocomial transmission in the Toronto SARS outbreak, *Math. Biosci. Eng.*, **1** (2004), 1–13. https://doi.org/10.3934/mbe.2004.1.1

AIMS Press